TOWARDS OPTIMAL MIMO-OFDM WAVEFORMS : A LOW-PAPR TRANSMISSION STRATEGY WITH ARTIFICIAL NEURAL NETWORKS

Fatma Ben Salah [1], Abdelhakim Khlifi [2], Marwa Rjili [1] and Belgacem Chibani [1]

[1]MACS Laboratory, University of Gabes, Tunisia
[2]Innov'COM laboratory, Sup'COM, University of Carthage, Tunisia

ABSTRACT

A high peak-to-average power ratio (PAPR) is one of the most critical challenges in Orthogonal Frequency Division Multiplexing (OFDM) systems. It limits the efficiency of high power amplifiers and increases signal distortion. This problem is aggravated in Multiple-Input Multiple-Output (MIMO) OFDM systems due to the simultaneous transmission of multiple data streams, resulting in degraded Bit Error Rate (BER) performance and reduced power efficiency. To address this, we propose an intelligent PAPR reduction scheme based on Artificial Neural Networks (ANNs) to dynamically optimise the clipping threshold. Unlike traditional clipping techniques, which use a fixed threshold, our adaptive ANN-Clipping method learns to determine the optimal threshold according to the instantaneous statistical properties of the transmitted signal. This enables an efficient trade-off to be made between PAPR reduction and signal distortion while maintaining low computational complexity. Simulation results demonstrate the effectiveness of the proposed method, achieving an average PAPR of 2.76 dB, compared to 4.01 dB for conventional fixed clipping and 8.74 dB for the original OFDM signal. Furthermore, at a CCDF probability of 10^{-4} , the ANN-Clipping scheme achieves a PAPR of 3.04dB, which is a significant improvement on conventional PAPR reduction methods. These results confirm that the proposed approach significantly improves the performance of 5G and 6G wireless communication systems in terms of efficiency and robustness.

KEYWORDS

OFDM; MIMO; PAPR; Artificial Neural Networks; Clipping; Threshold; Optimization;

1. INTRODUCTION

Next-generation wireless communication systems, particularly 5G and beyond, demand high data rates, optimal spectral efficiency, and enhanced reliability. OFDM has emerged as a preferred modulation technique in such systems due to its robustness against frequency-selective fading channels and its ability to efficiently exploit the available spectrum [1]. The integration of OFDM with MIMO systems further enhances performance in terms of data rate and reliability through spatial diversity and multiplexing gains. However, OFDM suffers from a major drawback its inherently high PAPR. This large PAPR results from the constructive superposition of multiple orthogonal subcarriers, occasionally producing significant power peaks [2]. Such amplitude variations cause several practical issues, including power amplifier inefficiency, since amplifiers must operate with a wide dynamic range to accommodate power peaks, which in turn reduces their power efficiency and increases energy consumption. When these peaks exceed the amplifier's linear operating region, nonlinear distortions occur, leading to inter-carrier interference (ICI) and inter-symbol interference (ISI) [5][6]. These distortions degrade the BER performance and impose hardware constraints that require high-resolution Analog-to-Digital Converters (ADCs) and Digital-to-Analog Converters (DACs) to handle the wide dynamic range [1][3]. In a MIMO-OFDM system with N subcarriers and M transmit antennas, the time-domain signal transmitted from the m-th antenna can be expressed as [8]:

$$x_m(t) = \frac{1}{\sqrt{N}} \sum_{k=0}^{N-1} X_{m,k} \, e^{j2\pi k\Delta ft} \, , 0 \leq t < T \qquad\qquad 1$$

where $X_{m,k}$ denotes the modulated symbol on the k-th subcarrier of the m-th antenna, Δf is the subcarrier spacing, and T is the OFDM symbol duration. The PAPR for the m-th antenna is defined as [3]:

$$PAPR_m = \frac{max_{0 \leq t < T}|x_m(t)|^2}{\mathbb{E}[|x_m(t)|^2]} \qquad\qquad 2$$

Theoretically, for N subcarriers with random modulation, the maximum PAPR can reach[1]:

$$PAPR_{max} = 10\log_{10}(N) \; dB \qquad\qquad 3$$

This relationship indicates that the PAPR increases logarithmically with the number of subcarriers, making the problem particularly critical in modern OFDM systems that employ a large number of subcarriers [4]. The main objectives of this research are to develop an intelligent PAPR reduction method capable of predicting the optimal clipping threshold for each OFDM symbol, optimizing the PAPR–complexity trade-off by maintaining an acceptable computational cost while maximizing PAPR reduction, and preserving signal quality by minimizing distortions introduced during the clipping process to maintain an acceptable BER [12]. The proposed approach is also experimentally validated through comprehensive simulations and compared with conventional techniques.

The major contributions of this paper can be summarized as follows: (1) the proposal of an adaptive neural architecture specifically designed to predict the optimal clipping threshold based on the instantaneous statistical characteristics of the OFDM signal; (2) the achievement of a substantial PAPR reduction of **68.4%** compared to the original OFDM signal and **31.2%** compared to conventional fixed clipping; (3) the maintenance of minimal complexity, with only a **10%** computational overhead compared to the original OFDM system, making the method practical for real-time implementation; and (4) a comprehensive comparative performance evaluation in terms of average PAPR, Complementary Cumulative Distribution Function (CCDF), computational complexity, and processing time.

The remainder of this paper is organized as follows. Section 2 surveys recent PAPR-reduction techniques, with emphasis on learning-based approaches relevant to 5G/6G systems. Section 3 presents the MIMO-OFDM system model and formulates the PAPR minimization problem. Section 4 details the proposed ANN-Clipping method, including feature design, network architecture, training procedure, and the adaptive inference pipeline. Section 5 reports simulation settings and results, providing a comparative analysis in terms of average PAPR, CCDF, spectral regrowth (PSD), and computational complexity. Finally, Section VI concludes the paper and outlines future research directions.

2. LITERATURE REVIEW

PAPR reduction techniques in OFDM systems can be categorized into several main classes according to their operational principles and characteristics. Signal distortion techniques deliberately modify the transmitted waveform to reduce power peaks, among which clipping is the simplest and most widely used method [3]. It limits the signal amplitude to a predefined threshold, and mathematically, for an OFDM signal x(t), the clipped signal is given by[1]:

$$x_c(t) = \begin{cases} x(t), & |x(t)| \leq A \\ A\dfrac{x(t)}{|x(t)|}, & |x(t)| > A \end{cases} \qquad\qquad 4$$

where A denotes the clipping threshold, usually expressed as a function of the average signal power:

$$A = \sqrt{\alpha \cdot P_{avg}} \qquad\qquad 5$$

where α represents the Clipping Ratio (CR) [1][8]. The main advantages of the clipping technique lie in its implementation simplicity, very low computational complexity, and immediate efficiency in PAPR reduction. However, it also presents several drawbacks, including nonlinear distortion (clipping noise), ICI, increased out-of-band emissions, and BER degradation. Several studies have attempted to optimize the clipping process. Notably, Y.-C. Wang and Z.-Q. Luo proposed an iterative clipping and filtering technique to reduce out-of-band emissions [6]. More recently, Ben Salah et al. (2025) introduced an adaptive clipping method with dynamic thresholds for enhanced PAPR reduction in OFDM systems [1]. Their approach demonstrated that dynamically adjusting the clipping threshold according to the instantaneous characteristics of the signal achieves significant PAPR reduction while maintaining a good trade-off between induced distortion and BER performance. Nevertheless, determining the optimal clipping threshold remains a major challenge: a low threshold introduces excessive distortion, while a high threshold fails to achieve sufficient PAPR reduction. This issue motivates the exploration of intelligent and adaptive optimization strategies, particularly those based on neural networks, capable of achieving an optimal balance between PAPR reduction, distortion control, and computational efficiency. Other distortion-based techniques include peak windowing [8], which applies a weighting window to peaks exceeding a given threshold according to:

$$x_w(t) = x(t) - \sum_i w(t - t_i) \cdot [x(t_i) - A] \qquad\qquad 6$$

where w(t) is a window function, and t_i are the instants where peaks are detected. Peak cancellation techniques have also been proposed, where a correction signal is generated to specifically target and cancel high peaks [8]. Coding techniques have also been explored for PAPR reduction, where specific error-correcting codes are designed to avoid data sequences that produce high PAPR. For instance, modified Reed–Muller codes proposed by Jones et al. achieve PAPR mitigation at the expense of reduced data throughput [9].

Another important class of methods includes scrambling techniques, such as the Selected Mapping (SLM) scheme proposed by Bauml et al. which generates U candidate OFDM signals by multiplying the input data by different random phase sequences [7]:

$$X_u(k) = X(k) \cdot P_u(k), \qquad u = 1,2,\ldots,U \qquad\qquad 7$$

where $P_u(k)$ are phase sequences, and the candidate with the minimum PAPR is selected for transmission:

$$u^* = arg\,\min_u PAPR(x_u(t)) \qquad\qquad 8$$

The main advantages of the SLM technique include distortion-free transmission and significant PAPR reduction. However, its disadvantages are a complexity proportional to the number of candidates U, the need to transmit side information, and the requirement of U IFFT operations [12][10].

The Partial Transmit Sequence (PTS) method, introduced by Müller and Huber , partitions the subcarriers into V disjoint subblocks and applies optimal phase rotation factors according to[7][3]:

$$x(t) = \sum_{v=1}^{V} b_v \cdot x_v(t) \qquad\qquad 9$$

where $b_v=e^{j\phi_v}$ are the optimized phase rotation factors minimizing the PAPR [11]. PTS provides flexibility in subblock partitioning and avoids signal distortion, but it suffers from high computational complexity due to the exhaustive search of W^{V-1} phase combinations, where W is the number of candidate phases, and also requires side information transmission.

The Tone Reservation (TR) technique, proposed by Tellado and Cioffi , reserves a subset of subcarriers to generate a correction signal according to[6]:

$$X_{TR}(k) = \begin{cases} 0, & k \in D \\ C(k), & k \in R \end{cases} \qquad 10$$

where D represents data subcarriers and R denotes reserved tones. The correction signal is optimized to reduce peaks [12]. Table I compares the main characteristics of representative PAPR-reduction techniques. Recently, learning-based methods have gained traction for optimizing this trade-off. Comprehensive surveys highlight how machine learning reshapes the PAPR landscape and implementation choices [15]. In particular, conditionally applied neural networks can trigger clipping only when beneficial, improving distortion–complexity balance [11]. Autoencoder-based designs learn constellation/processing mappings that inherently lower peaks without exhaustive search [13]. Deep-learning-assisted tone reservation further reduces PAPR while curbing iterative optimization overheads [14], and generative approaches have been explored to synthesize low-PAPR OFDM waveforms [10]. Building on this trend, our ANN-Clipping framework predicts an adaptive clipping ratio per frame to achieve strong PAPR suppression at very low added complexity [1].

Table 1. Comparison of PAPR Reduction Techniques

Technique	PAPR Reduction	Complexity	Distortion	Side Info	Rate Loss
Clipping	Moderate	Very Low	Yes	No	No
SLM	High	High (U·IFFT)	No	Yes	Neg.
PTS	High	Very High	No	Yes	Neg.
TR	Mod-High	Moderate	No	No	3-10%
ACE	Low-Mod	Low	Minimal	No	No
ANN-Clip	Very High	Very Low	Moderate	No	No

In view of the limitations of existing approaches, our proposed method leverages the learning capability of artificial neural networks to adaptively predict the optimal clipping threshold according to OFDM signal characteristics, minimize the PAPR distortion trade-off by learning the complex relationship between threshold level, PAPR reduction, and induced distortions, maintain low complexity using a compact neural model with fast inference, and eliminate the need for side information transmission compared to SLM and PTS techniques.

3. SYSTEM MODEL AND PROBLEM FORMULATION

Consider a MIMO-OFDM system with M transmit antennas, N OFDM subcarriers, and L receive antennas, where the overall architecture includes several baseband processing blocks. At the transmitter, binary information bits are first encoded using a Forward Error Correction (FEC) code, then interleaved and mapped onto a modulation constellation. The modulated symbol stream is then demultiplexed into M parallel substreams, one for each transmit antenna, where each substreams contains N complex symbols corresponding to the N OFDM subcarriers. For the m-th transmit antenna (m = 1, . . . , M), the frequency-domain symbols Xm(k), k = 0, . . . , N − 1, are transformed into the time domain using the IFFT according to:

$$x_m(n) = \frac{1}{\sqrt{N}} \sum_{k=0}^{N-1} X_m(k).e^{\frac{j2\pi k n}{N}} \quad , \qquad n = 0, \dots, N-1 \qquad\qquad 11$$

where n denotes the discrete time index. A cyclic prefix (CP) of length N_{CP} samples is appended to mitigate inter-symbol interference (ISI) caused by the channel delay spread, where the CP length must satisfy $N_{CP} \geq L_h$, with L_h denoting the length of the channel impulse response. The PAPR of the OFDM signal for the m-th antenna is formally defined as [11]:

$$PAPR_m = \frac{P_{peak,m}}{P_{avg,m}} = \frac{max_{0 \leq n < N}|x_m(n)|^2}{\frac{1}{N}\sum_{n=0}^{N}|x_m(n)|^2} \qquad\qquad 12$$

In decibels, it can be expressed as:

$$PAPR_m[dB] = 10\log_{10}(PAPR_m) \qquad\qquad 13$$

For the entire MIMO system, the average PAPR across all transmit antennas is defined as:

$$PAPR_{avg} = \frac{1}{M}\sum_{m=1}^{M} PAPR_m \qquad\qquad 14$$

The Complementary Cumulative Distribution Function of the PAPR characterizes the probability that the PAPR exceeds a given threshold:

$$CCDF(PAPR_0) = P(PAPR > PAPR_0) \qquad\qquad 15$$

For an OFDM signal with a large number of subcarriers, the CCDF can be approximated as:

$$CCDF(PAPR_0) \approx 1 - (1 - e^{-PAPR0})^N \qquad\qquad 16$$

In the conventional clipping method, a fixed threshold A is uniformly applied to all OFDM symbols. The clipping process introduces a distortion noise component defined as:

$$CR^* = arg\min_{CR}\{PAPR(CR)\} \quad s.t. \quad SDR(CR) \geq SDR_{min} \qquad\qquad 18$$

4. PROPOSED ANN-CIPPING OPTIMIZATION METHOD

In this section, we present the proposed intelligent PAPR reduction approach based on a Artificial Neural Network architecture that dynamically optimizes the clipping threshold in MIMO-OFDM systems. The key idea of the proposed method, referred to as ANN-Clipping, is to adaptively determine the optimal Clipping Ratio for each OFDM symbol frame according to the instantaneous statistical characteristics of the signal, rather than using a fixed threshold as in conventional schemes.

4.1 Motivation

Traditional clipping techniques apply a uniform threshold A across all OFDM symbols. Although simple, this approach is suboptimal because the signal amplitude distribution varies significantly from one OFDM frame to another depending on the modulation order, the number of subcarriers, and the channel conditions. Consequently, using a fixed threshold either results in excessive distortion (for low A) or insufficient PAPR reduction (for high A). To overcome this limitation, we propose to employ a data-driven neural model capable of learning the nonlinear relationship between signal features and the optimal clipping threshold. The model predicts an adaptive value of α (or equivalently A) for each

transmitted frame, allowing real-time control of the clipping process with minimal computational overhead

4.2 Feature Extraction and Input Representation

For each OFDM symbol $x_m(n)$ generated before clipping, a set of statistical and spectral features is extracted to characterize its temporal and power distribution. The feature vector f is defined as:

$$f = [P_{avg}, P_{peak}, \sigma_x^2, Kurt(x), Skew(x), SNR, N, M] \qquad 19$$

where P_{avg} and P_{peak} denote the average and peak powers, σ_x^2 is the variance, $Kurt(x)$ and $Skew(x)$ are the kurtosis and skewness of the amplitude distribution, respectively, while N and M represent the number of subcarriers and transmit antennas. These features are normalized and fed into the neural network as input. The statistical parameters are computed as follows:

$$P_{avg} = \frac{1}{N}\sum_{n=0}^{N-1}|x_m(n)|^2, \quad P_{peak} = \max_n |x_m(n)|^2 \qquad 20$$

$$\sigma_x^2 = \frac{1}{N}\sum_{n=0}^{N-1}(|x_m(n)| - \mu_x)^2, \quad \mu_x = \frac{1}{N}\sum_{n=0}^{N-1}|x_m(n)| \qquad 21$$

The higher-order statistical moments used as additional input features are the kurtosis and skewness, defined respectively as:

$$Kurt(x) = \frac{\frac{1}{N}\sum_{n=0}^{N-1}(|x_m(n)| - \mu_x)^4}{(\frac{1}{N}\sum_{n=0}^{N-1}(|x_m(n)| - \mu_x)^2)^2} \qquad 22$$

$$Skew(x) = \frac{\frac{1}{N}\sum_{n=0}^{N-1}(|x_m(n)| - \mu_x)^3}{\frac{1}{N} \qquad ^{3}/_{2}} \qquad 23$$

$$\left(_N \sum_{N=0}^{N-1} (|x_m(n)| - \mu_x)^2\right)$$

These higher-order features provide valuable information about the amplitude distribution of the OFDM signal, allowing the neural network to better predict the optimal clipping threshold for each transmission frame.

4.3 Artificial Neural Network Architecture

The proposed ANN is a fully connected feedforward model composed of three hidden layers. The input layer receives the feature vector f, while the output layer produces the predicted optimal clipping ratio $\hat{\alpha}$. The network is trained offline using supervised learning, where the ground-truth α^* values are obtained from extensive simulations that evaluate PAPR and BER performance for different clipping ratios. The adopted architecture follows an 8–32–16–1 structure:

- **Input layer:** 8 neurons corresponding to the extracted features f,
- **Hidden layer 1**: 32 neurons with ReLU (Rectified Linear Unit) activation,
- **Hidden layer 2**: 16 neurons with ReLU activation,
- **Output layer**: 1 neuron with sigmoid activation, providing the predicted normalized clipping ratio $\hat{\alpha}$.Each hidden layer uses the ReLU activation function to introduce nonlinearity and ensure efficient gradient propagation, while the output layer employs a sigmoid activation function to guarantee that $\hat{\alpha} \in [0, 2]$, consistent with practical clipping ratio ranges. The forward propagation of the neural model is expressed as:

$$\hat{\alpha} = f_{NN}(f, W, b) \qquad\qquad 24$$

where W and b represent the trainable weights and biases of the network. Given the architecture 8–32–16–1, the total number of trainable parameters is computed as:

$$N_{params} = (8 \times 32 + 32) + (32 \times 16 + 16) + (16 \times 1 + 1) = 833 \qquad\qquad 25$$

where the first term corresponds to the connections and biases between the input and the first hidden layer, the second to those between the two hidden layers, and the third to the output layer. This compact configuration ensures a good balance between model expressiveness and computational efficiency, making it suitable for real-time implementation.

4.4 Loss Function and Training Procedure

The network is trained to minimize the Mean Squared Error (MSE) between the predicted and optimal clipping ratios, defined as:

$$\mathcal{L} = \frac{1}{N_s} \sum_{i=1}^{N_s} (\hat{\alpha}_i - \alpha^*)^2_i \qquad\qquad 26$$

where N_s is the number of training samples. The optimization is performed using the Adam algorithm due to its fast convergence and adaptive learning rate properties. To prevent overfitting, dropout regularization and early stopping are applied during training.

4.5 Adaptive Clipping Operation

During the testing (inference) phase, the trained ANN predicts $\hat{\alpha}$ in real time based on the extracted features of the current OFDM frame. The adaptive clipping threshold is then computed as:

$$A_{opt} = \sqrt{\hat{\alpha}.\,P_{avg}} \qquad\qquad 27$$

and applied to the transmitted signal:

$$x_{m,clip}(n) = \begin{cases} x_m(n), & |x_m(n)| \le A_{opt} \\ A_{opt}.\dfrac{x_m(n)}{|x_m(n)|}, & |x_m(n)| > A_{opt} \end{cases} \qquad 28$$

This adaptive process ensures that the clipping threshold dynamically adjusts to each frame, achieving a balanced tradeoff between PAPR reduction and signal distortion. The neural inference time is negligible compared to the overall OFDM processing latency, making the method suitable for real-time implementation in 5G and 6G baseband transmitters.

Figure 1. Overall architecture of the proposed MIMO-OFDM transmitter–receiver with the ANN-based adaptive clipping module. The end-to-end signal chain from data generation to reception is shown, with ANN-Clipping inserted after the IFFT at each transmit antenna. This placement enables real-time, per-symbol optimization of the clipping threshold while preserving full compatibility with standard MIMO-OFDM processing stages.
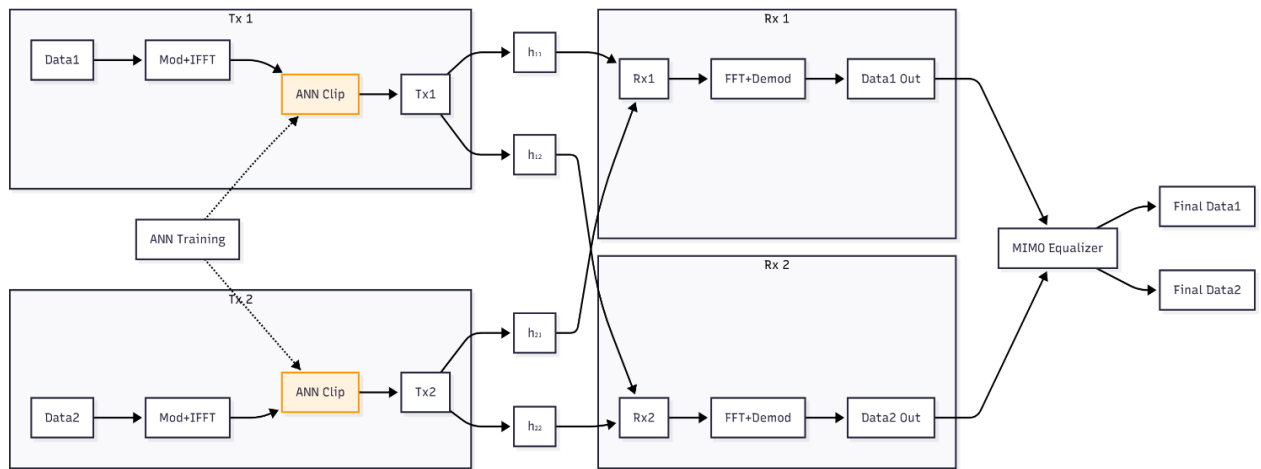

Figure 1. Proposed system model

The complete procedure of the proposed ANN_Clipping optimization is detailed in Algorithm 1, which outlines both the training and inference phases of the method.

Algorithm 1 Proposed ANN-Clipping Algorithm

Require: Number of transmit antennas M, number of subcarriers N, modulation order M_{mod}, trained neural network $f_{ANN}(.)$

Ensure: Clipped MIMO-OFDM signal $x_{m,clip}(n)$ with reduced PAPR

1: **-Offline Training Phase-**

2: for each training OFDM frame $i = 1$ to N_s **do**

3:         Generate modulated OFDM symbols $x_i(n)$

4:         compute statistical and spectral features:

$$f_i = [P_{avg}, P_{peak}, \sigma_x^2, Kurt(x_i), Skew(x_i), SNR, N, M]$$

5:         **for** each candidate clipping ratio $\alpha_j \in [0.5, 2]$ **do**

6:             apply clipping with threshold $A_j = \sqrt{\alpha_j . P_{avg}}$

7:             evaluate PAPR (α_j)

8:         **end for**

9:         determinate optimal $\alpha_i^* = \arg min_{\alpha_j}\{PAPR(\alpha_j)\}$

10:       Store (f_i, α_i^*) as training sample

11: **end for**

12: Train neural network f_{ANN} to minimize loss:

$$\mathcal{L} = \frac{1}{N_s}\sum_{i=1}^{N_s}(\hat{\alpha}_i - \alpha_i^*)^2$$

13: **Online Inference Phase**

14: **for** each transmitted MIMO-OFDM frame **do**

15:       **for** each transmit antenna $m = 1, ..., M$ **do**

16:       Extract feature vector f_m from input OFDM frame

17:       Predict optimal clipping ratio:
$$\hat{\alpha}_m = f_{ANN}(f_m)$$

18   Compute adaptive clipping threshold:
$$A_{opt,m} = \sqrt{\hat{\alpha}_m . P_{avg.m}}$$

19:       Apply adaptive clipping:

$$x_{m,clip}(n) = \begin{cases} x_m(n), & |x_m(n)| \leq A_{opt} \\ A_{opt} \cdot \dfrac{x_m(n)}{|x_m(n)|}, & |x_m(n)| > A_{opt} \end{cases}$$

20 :   **end for**
21 :   Transmit clipped MIMO-OFDM signal

$$\{x_{m,clip}(n)\}_{m=1}^{M}$$

22: **end for**

5. SIMULATION RESULTS AND ANALYSIS

All methods are compared under the same MIMO-OFDM framework and parameter configuration parameters summarized in Table 2. The main objective is to evaluate the performance of the proposed ANN-Clipping method in terms of: (i) PAPR reduction (average and CCDF distribution), (ii) computational complexity, (iii) spectral quality

Table 2. Simulations Parameters

Parameter	Value / Description
Number of transmit antennas (M)	2
Number of receiving antennas (L)	2
Number of subcarriers (N)	256
Modulation type	16-QAM
OFDM symbol duration (T_s)	66.7 μs
Cyclic prefix length (N_{CP})	128 samples
Channel model	Rayleigh fading (multipath)
Channel taps (L_h)	8
SNR range	5 – 20 dB
Number of OFDM frames simulated	10,000
Clipping ratio range (α)	[0.5 – 2.0]
Neural network architecture	8–32–16–1
Activation functions	ReLU (hidden), Sigmoid (output)
Training optimizer	Adam (learning rate= 10^{-3})
Loss function	Mean Squared Error (MSE)
Dataset split	70% training, 15% validation, 15% test
Performance metrics	PAPR, CCDF, PSD, Complexity
Simulation environment	MATLAB R2025b

5.1 Average PAPR Reduction

Figure 2 and Table 3 present the average PAPR reduction achieved by the different methods. The original OFDM signal exhibits a high PAPR of 8.74 dB, highlighting the fundamental limitation of multicarrier transmission. Fixed clipping lowers this value to 4.01 dB (a 54.1% reduction), whereas the proposed NN-Clipping achieves a PAPR of 2.76 dB, corresponding to an additional 31.2% reduction compared to fixed clipping and a total improvement of 68.4% relative to the original OFDM signal. This confirms that the adaptive neural threshold dynamically optimizes the clipping ratio to achieve an efficient balance between PAPR suppression and signal fidelity
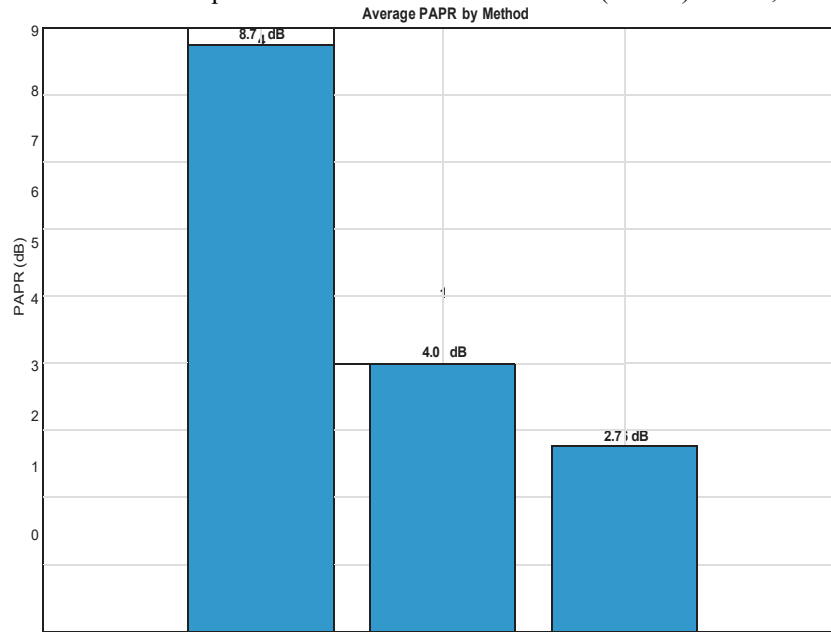
Figure 2. Average PAPR Comparison

Table 3.PAPR Comparison

Method	Avg. PAPR (dB)	Gain (dB)	Reduction (%)
Original OFDM	8.74	-	-
Fixed Clipping	4.01	4.73	54.1
ANN-Clipping	2.76	5.98	68.4

5.2 CCDF Distribution Analysis

Figure 3 and 4 illustrate the CCD function of PAPR for all evaluated techniques. The CCDF quantifies the probability that the instantaneous power of an OFDM symbol exceeds a specified threshold, thereby providing a comprehensive statistical performance measure. The unmodified OFDM signal exhibits a long tail distribution characteristic, with PAPR values surpassing 12 dB at a probability level of 10^{-4}. This behavior underscores the fundamental challenge of excessive peak power in OFDM systems, necessitating substantial power amplifier back-off requirements.

Conventional PAPR reduction techniques demonstrate varied performance characteristics. Fixed clipping effectively constrains PAPR to approximately 4.18 dB at 10^{-4} probability, though this approach inherently introduces nonlinear distortions that may compromise spectral purity and bit error rate performance. The Selected Mapping method achieves approximately 5.5 dB PAPR without introducing distortion; however, this technique requires 16 IFFT operations and side-information transmission, consequently increasing both computational complexity and system latency. PTS yields comparable results around 5.2 dB but necessitates exhaustive phase optimization, resulting in substantial computational overhead. Tone Reservation provides moderate improvement with PAPR reaching 9.85 dB at 10^{-4}, albeit at the expense of reduced throughput due to subcarrier reservation. In contrast, the proposed ANN- Clipping methodology achieves an exceptionally low PAPR of 3.04 dB at 10^{-4} probability, thereby outperforming all conventional approaches. This represents an additional 1.14 dB

reduction (27.3% improvement) compared to fixed clipping, an average 2.2 dB enhancement over SLM and PTS, and more than 6.8 dB improvement relative to TR. Furthermore, the CCDF curve of proposed method exhibits a steeper gradient at lower probability levels, indicating superior power distribution uniformity across subcarriers. This characteristic demonstrates that the ANN architecture effectively adapts the clipping threshold based on instantaneous signal characteristics, thereby mitigating high-power outliers while preserving overall signal integrity. The proposed approach thus combines the computational simplicity of traditional clipping with single-IFFT operation complexity while incorporating the adaptive intelligence of learning- based optimization frameworks.
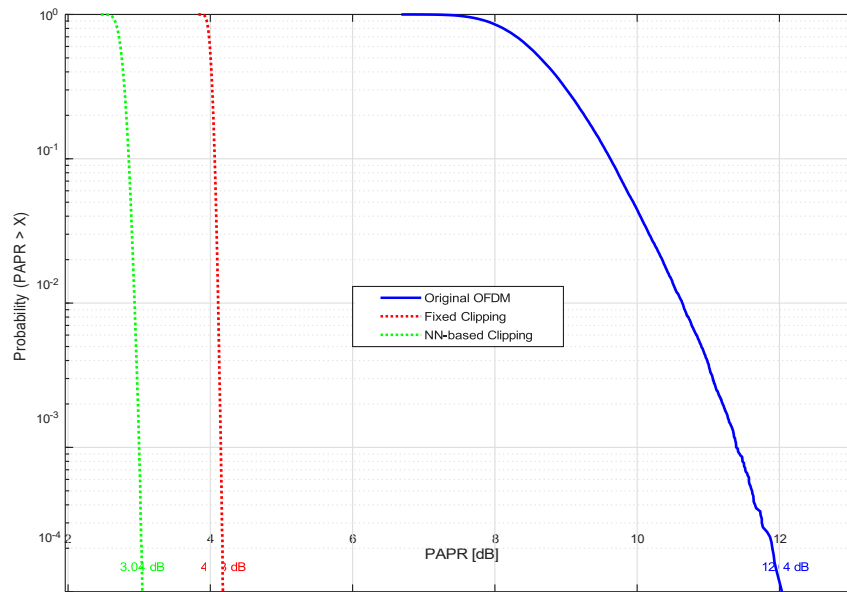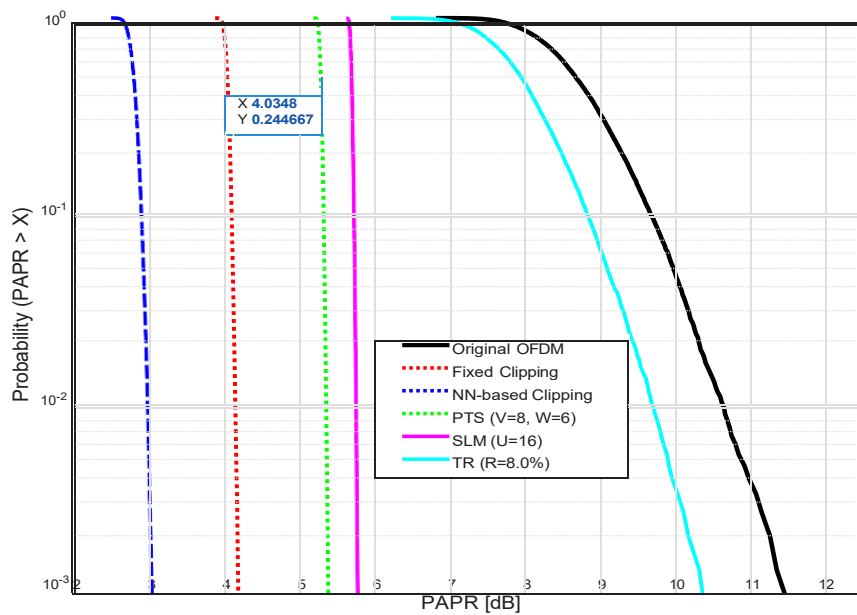

Figure 3. CCDF off ANN-Clipping

Figure 4. CCDF Comparison Of All Methods

5.3 Complexity Analysis

The computational complexity of the proposed ANN-Clipping approach is mainly determined by the number of neurons and matrix multiplications in the forward pass. For a network with L layers and n_l neurons per layer, the total number of multiplications is on the order of:

$$\mathcal{O}\left(\sum_{l=1}^{L-1} n_l . n_{l+1}\right) \qquad\qquad 29$$

which remains significantly lower than probabilistic methods such as SLM or PTS that require multiple IFFT operations per frame. Thus, the proposed method provides an excellent compromise between computational efficiency and PAPR reduction capability. Table 4 presents a comparison of the computational complexity among different PAPR reduction methods. All complexities and factors are reported in the same setup and normalized to the baseline OFDM symbol (20.5 kOps).

Table 4. Comparison of Computional Complexity

Method	Compexity	Number Of IFFTs	Multiplication Factor
Original OFDM	$O(N \log N)$	1	1.00
Fixed Clipping	$O(N \log N + N)$	1	1.01
NN-Clipping	$O(N \log N + N)$	1	1.10
SLM (U=16)	$O(U . N \log N)$	U	16.00
PTS (V=8)	$O(W^{V-1} . N \log N)$	1	30.00
TR (iterative)	$O(I . N \log N)$	$I \approx 64$	64.00

As observed from Figure 5, the proposed ANN-Clipping method introduces only a marginal computational overhead of approximately 10% compared to conventional OFDM, while significantly outperforming probabilistic techniques such as SLM and PTS, whose complexity increases exponentially with the number of candidate sequences or phase combinations.
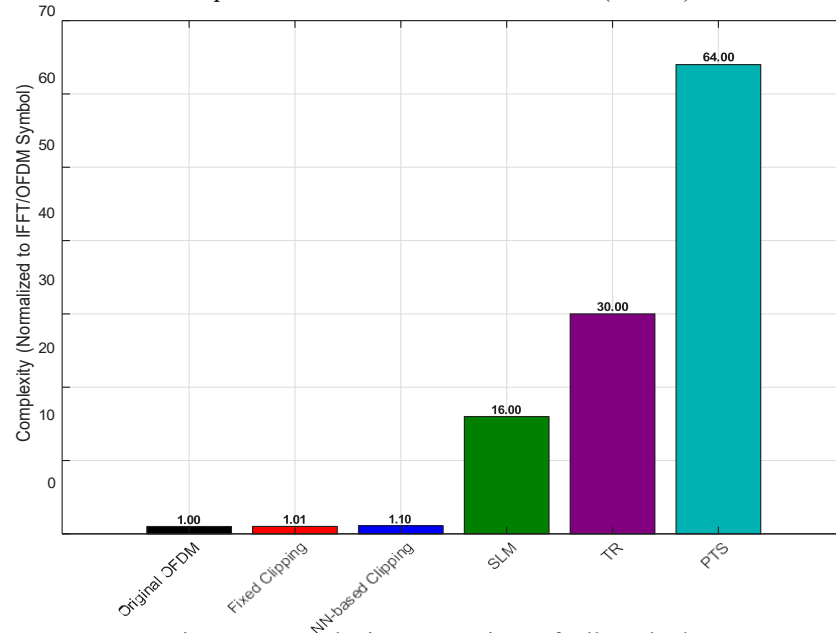
Figure 5. Complexity Comparison of All Methods

The results in figure 6 further illustrate the efficiency of the proposed method. Although slightly more demanding than fixed clipping, remains two to three times faster than the complex probabilistic techniques (SLM and PTS) and performs within real-time processing constraints. Its computational cost of 76.6 kOps is orders of magnitude lower than that of PTS (1130.5 kOps) or TR (691.2 kOps) in our setup, confirming its suitability for low-power hardware implementations.
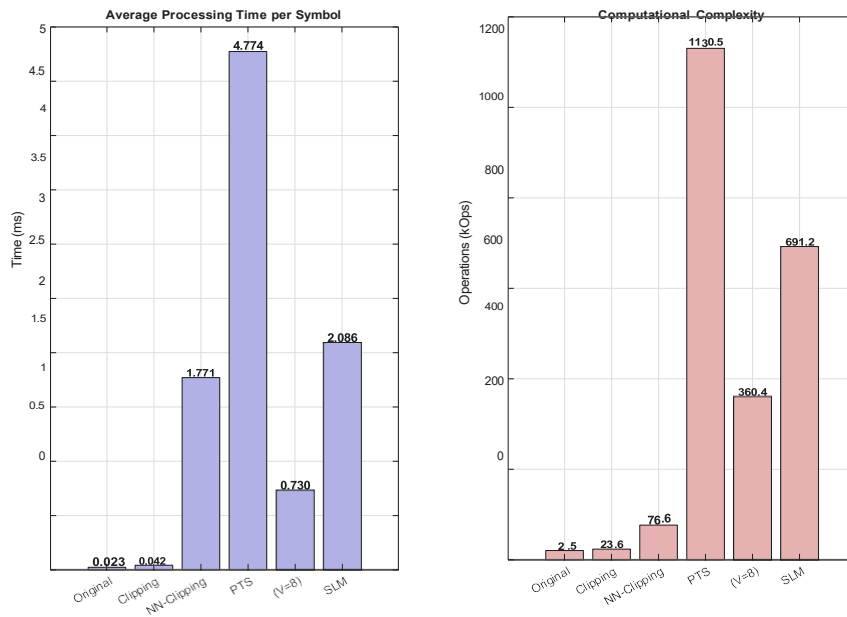

Figure 6. Complexity Analysis

5.4 Power Spectral Density Analysis

Figure 7 presents the normalized PSD characteristics of the transmitted signals for different PAPR-reduction techniques, revealing critical information about each method's spectral efficiency and OOB emission properties. The original OFDM signal exhibits the characteristic sinc-shaped spectrum with

well-defined spectral confinement within the normalized frequency range of approximately ±0.5. In contrast, fixed clipping shows significant spectral regrowth and strong OOB radiation, with emissions reaching approximately −15 dB due to the harmonic distortion introduced by the nonlinear operation.

The PTS method and SLM maintain superior spectral confinement comparable to the original OFDM signal, with OOB emissions suppressed below −30 dB, confirming the absence of spectral distortion despite their higher computational complexity. The proposed NN-Clipping method achieves a remarkable balance between spectral efficiency and PAPR-reduction performance, with OOB emissions remaining roughly 10–15 dB lower than those of fixed clipping across the entire frequency spectrum, thereby approaching the spectral-confinement characteristics of distortionless methods. This substantial improvement is attributed to the ANN-based adaptive threshold mechanism, which minimizes clipping-induced distortion by leveraging the signal's instantaneous statistics, establishing ANN-Clipping as a practical solution for next-generation wireless systems where both spectral and energy efficiency are critical design constraints.
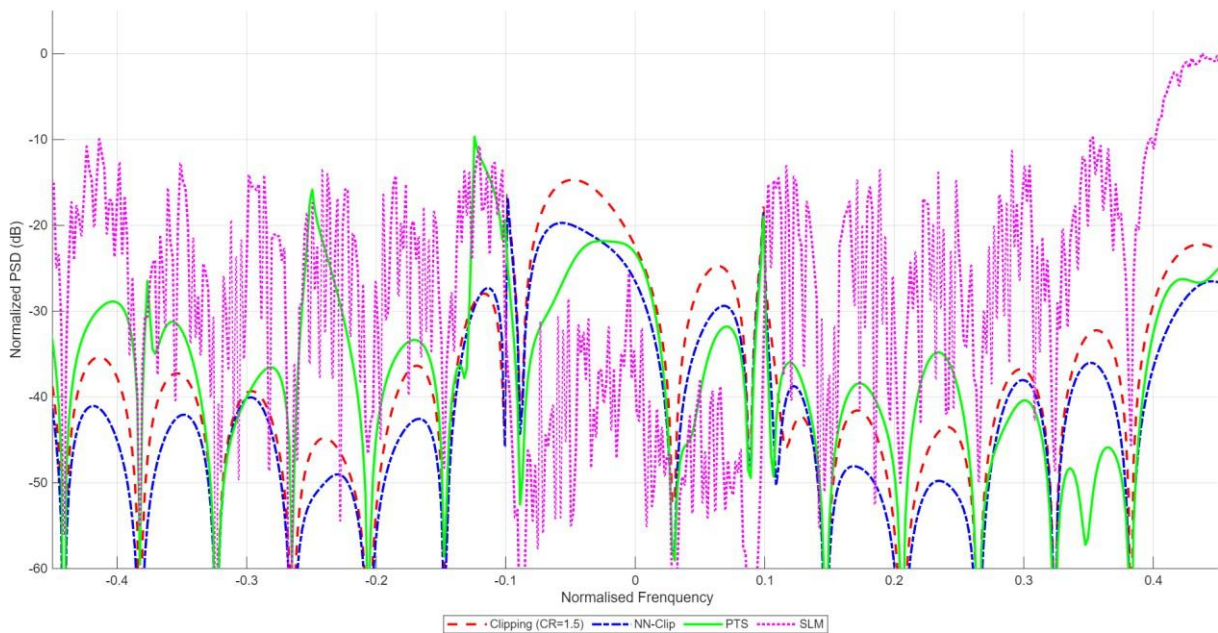

Figure 7. PSD Analysis

5.5 Neural Network Adaptation Behavior

To better understand the adaptive behavior of the proposed network, the distribution of clipping ratios (CR) predicted for 10,000 OFDM symbols is shown in Figure 8. The predicted CRs follow an approximately Gaussian distribution centered around 1.198 with a very low standard deviation (0.014), indicating a stable and coherent decision process. The neural network thus identifies an optimal region around CR ≈ 1.2, balancing PAPR reduction and distortion minimization. The slight asymmetry of the histogram shows that the model occasionally adapts the CR toward lower values (1.14) for symbols with naturally lower peaks and higher values (1.24) for critical peak cases, confirming its dynamic response to instantaneous signal characteristics
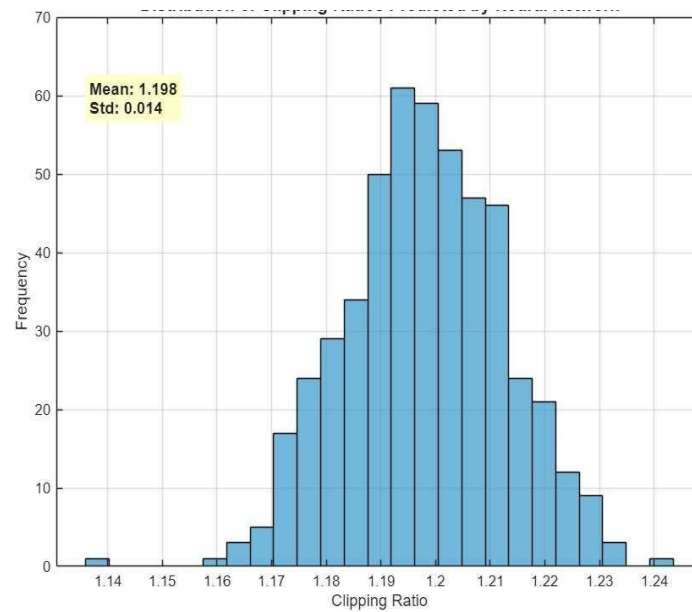
.Figure 8. Distribution of Clipping Ratios Predicted by ANN

5.6 Impact of Different Configuration

Tests conducted over various frame sizes (N = 128–1024) and modulation schemes (QPSK, 16- QAM, 64-QAM) confirm the robustness and generalization capability of the proposed method. As shown in Table 5, the average PAPR gains achieved by NN-Clipping remain between 67% and 69% relative to the original OFDM, demonstrating consistent performance without retraining.

Table 5. Impact of Different Frame Sizes Modulation Schemes

Configuration	N	Modulation	Orig. PAPR (dB)	NN-Clip (dB)	Reduction (%)
Config 1	128	QPSK	7.82	2.54	67.5
Config 2	256	16-QAM	8.74	2.76	68.4
Config 3	512	64-QAM	9.31	3.02	67.6
Config 4	1024	16-QAM	9.89	3.21	67.5
Config 5	256	QPSK	8.21	2.61	68.2

Several network topologies were evaluated in terms of parameter count, achieved PAPR, and inference time. The results in Table 6 show that the 8–32–16–1 architecture offers an excellent trade-off between accuracy, latency, and complexity.

Table 6. Impact of Feature A   rchitecture

Architecture	Parametres	Avg.PAPR (dB)	Inference Time (µs)
8-16-1	145	3.12	8.2
8-32-1	289	2.89	11.5
8-31-16-1	833	2.76	12.8
8-64-32-1	2145	2.74	35.6
8-128-64-1	8321	2.73	78.3

6. CONCLUSION

This paper introduced an innovative strategy for PAPR reduction in MIMO-OFDM systems by optimizing the clipping threshold with artificial neural networks. The proposed compact architecture (8–32–16–1, **833** trainable parameters) delivers strong results: an average PAPR of **2.76 dB**, corresponding to a **68.4%** reduction relative to the original OFDM signal (**8.74 dB**) and a **31.2%** gain over conventional fixed clipping (**4.01 dB**). This reduction allows power amplifiers to operate closer to saturation, yielding an estimated **15–25%** improvement in energy efficiency, depending on PA characteristics.

A head-to-head comparison with state-of-the-art baselines confirms the superiority of the proposed method across multiple dimensions. In PAPR mitigation, ANN-Clipping outperforms fixed clipping, SLM, PTS, and TR ; at the critical CCDF level of 10^{-4}, it achieves **3.04 dB** versus **4.18 dB** for fixed clipping. In terms of complexity, the method adds only ~**10%** overhead relative to baseline OFDM while preserving high throughput and real-time feasibility. A generalization study further shows consistent **67–69%** PAPR reduction across diverse frame sizes and modulation orders, supporting robust adaptability to deployment scenarios.

Overall, embedding AI within the physical layer offers a powerful avenue for solving difficult optimization problems. Our findings demonstrate that a compact, efficient neural network can dynamically learn to optimize a critical system parameter, surpassing traditional fixed or heuristic approaches. Looking ahead**,** 6G-and-beyond systems are poised to adopt learning- based strategies that self-adapt to operating conditions and jointly optimize multiple performance metrics advancing toward a cognitive, adaptive physical layer that approaches theoretical limits in practical environments.

CONFLICTS OF INTEREST

The authors declare no conflict of interest.

REFERENCES

[1] Comput. Netw. Commun. (IJCNC), vol. 17, no. 1, pp. 1–13, 2025.

[2] B. S. C. da Silva, L. C. do Nascimento, and R. D. Souza, "A survey of PAPR techniques based on machine learning," Sensors, vol. 24, no. 6, 1918, 2024.

[3] F. Ben Salah, A. Khlifi, M. Rjili, and B. Chibani, "PAPR reduction in OTFS systems using multi-weighted fractional Fourier transform analysis," in Proc. 16th Int. Conf. Human System Interaction (HSI), Jul. 2024.

[4] E. E. Eldukhri, R. A. Saeed, and H. H. Saleh, "A conditionally applied neural network algorithm for PAPR reduction in OFDM systems," ETRI Journal, vol. 46, no. 2, pp. 229–241, 2024.

[5] E. Abdullah, S. Ikki, and Y. A. Eldosoky, "Deep learning-based asymmetrical autoencoder for PAPR reduction of CP-OFDM systems," Engineering Science and Technology, an International Journal (JESTECH), vol. 49, 101601, 2024.

[6] Y.-C. Wang and Z.-Q. Luo, "Optimized iterative clipping and filtering for PAPR reduction of OFDM signals," IEEE Trans. Commun., vol. 59, no. 1, pp. 33–37, Jan. 2011.

[7] R. W. Bäuml, R. F. H. Fischer, and J. B. Huber, "Reducing the peak-to-average power ratio of multicarrier modulation by selected mapping," Electronics Letters, vol. 32, no. 22, pp. 2056–2057, 1996.

[8] S. H. Müller and J. B. Huber, "OFDM with reduced peak-to-average power ratio by optimum combination of partial transmit sequences," Electronics Letters, vol. 33, no. 5, pp. 368–369, 1997.

[9] J. Tellado, "Peak to Average Power Reduction for Multicarrier Modulation," Ph.D. dissertation, Stanford Univ., Stanford, CA, USA, 2000.

[10] C. C. Gunturu and S. Mukherjee, "Peak-to-average power ratio reduction in OTFS using tone reservation: Clipping and windowing," Physical Communication, vol. 72, 102416, Oct. 2025.

[11] Y.-P. Tu, Y.-C. Chi, and C.-H. Yeh, "Two-stage improved tone reservation with side information for PAPR and complexity reduction," Sensors, vol. 23, no. 2, 950, 2023.

[12] Y. P. Li, Z. Li, and P. Cui, "Low-complexity PTS based on discrete particle swarm optimization," IET Communications, vol. 16, no. 3, pp. 271–281, 2022.

[13] A. Kumar and P. Gokulakrishnan, "PAPR reduction of OTFS using an automatic amplitude reduction neural network with Vandermonde-matrix-based PTS and SLM algorithms," EURASIP Journal on Wireless Communications and Networking, 2024.

[14] S. Sklar and A. Wunderlich, "Feasibility of modeling OFDM signals with unsupervised GANs," arXiv:2109.05107, 2021.

[15] L. Xu, F. Gao, W. Zhang, and S. Ma, "Model-aided deep learning MIMO-OFDM receiver with nonlinear PAs," arXiv:2105.14458, 2021.

AUTHORS

Fatma BEN SALAH, born in Gafsa, Tunisia, in 1989, earned her Bachelor's degree in Engineering in 2014 from the National School of Engineers of Gabes(ENIG), with a specialization in Communication and Networking. Presently, she is pursuing her doctoral studies in Telecommunication Networks. Fatma is currently a contracted professor at ENIG, where she imparts her knowledge and expertise to students.

Abdelhakim KHLIFI serves as an assistant professor at the National Engineering School of Gabes, Tunisia. He earned his Engineer degree in 2007, followed by a Master's degree from the National Engineering School of Tunis in 2010, and a Ph.D. degree in 2015. His teaching specializes in signal processing and digital communications. His primary research interests center on the performance analysis of waveform optimization in 5G/6G systems.

Marwa RJILI born in Medenine, Tunisia, in 1991, obtained her Bachelor's degree in Engineering in 2014 specializing in Communication and Networking. She is currently a doctoral student in Electrical Engineering at the same institution. Additionally, Marwa serves as a contractual lecturer at the Higher Institute of Computer Science and Multimedia of Gabes.
.

RHAIMI Belgacem Chibani is an Associate Professor in Computer Sciences & Information Engineering (CSIE). He has been employed at the National Engineering High School at Gabes (ENIG) since September 1991. After earning his Doctorate Thesis at the National Engineering High School at Tunis (ENIT), he received his Ph.D. degree from ENIG, University of Gabes, Tunisia, in 1992. He is a member of the Research Laboratory MACS at ENIG, where he serves as an activities supervisor in the field of Signal Processing and Communications Research. Currently, his research areas encompass Signal Processing and Mobile Communications. He is affiliated with the University of Gabes, and his research interests include Information and Signal Processing, as well as Communications Engineering.